Neural Network Control of Robot under Wheel Slip Conditions based on Observer

Linghong Zhu, Xiaochen Huang, Xiaoming Wu, Rui Chen, Dajian Yi, Wenhui Zhang

Abstract: **For the complex control issues such as tire slippage, uncertain model parameters, and external disturbances in wheeled mobile robots (WMRs), a novel control approach based on observer-based fuzzy wavelet neural networks (FWNN) is proposed. To address the distortion of angular velocity information caused by tire slippage, mathematical equations for tire slippage and attitude deviation are utilized to design a sliding-mode observer for real-time estimation of angular velocity information. Considering the uncertainties in parameters and unknown model components due to external disturbances, a FWNN is designed to dynamically compensate for these uncertainties using expert knowledge from fuzzy systems and the generalization capability of wavelet neural networks (WNN). To ensure bounded control signals and system stability, a robust controller for the neural network is developed based on H∞ theory, and the asymptotic stability of the entire closed-loop system is proven using Lyapunov theory. Experimental results validate the effectiveness of the proposed control algorithm.**

Keywords: **Mobile robots; Wheel slip; Sliding mode observer; Neural networks; H∞ theory**

I. INTRODUCTION

With the development of robot application technologies [1-4], wheeled mobile robots (WMRs) have gradually entered various domains, including assembly handling, home services, disaster relief, planetary exploration, and various military applications. However, when mobile robots operate in complex environments such as wet and slippery surfaces or during rapid turns, the assumption of pure rolling of the wheels becomes invalid due to wheel slippage. Consequently, studies based on this assumption fail to meet the requirements, resulting in accumulation of pose errors and a significant decrease in the motion accuracy of mobile robots.

Many scholars have conducted research on the phenomenon of wheel slip in mobile robots. Moosavian et al. [5] considered the relationship between slip and trajectory radius, obtaining the slip parameters in the form of an exponential function of the path curvature radius. Gracia et al. [6] integrated the traction force model of wheel slip and utilized a weighted least squares algorithm to establish a connection between the non-slip kinematic equations of WMR and the slip modeling equations. Muir et al. [7] employed axle encoder readings for real-time computation of robot position to prevent excessive slipping and devised feedback control algorithms utilizing sensor data for real-time robot control. These scholars primarily focused on wheel slip at the kinematic level, where the kinematic model only considers position and velocity. Therefore, this paper introduces a dynamic model based on kinematics, while considering factors such as model uncertainty, unmodeled or unstructured disturbances. Nandy et al. [8] established a dynamic model for nonholonomic mobile robots considering constraints of both slipping and non-slipping, and proposed transition conditions between them. Through simulation combining the traction force model and system dynamics equations, the effectiveness of the method was validated. Wang et al. [9] proposed an active control method to adjust the vertical forces of the wheels on the ground by manipulating the pose of a manipulator on the mobile base to exert greater force and prevent slipping. However, the effectiveness of this method, which adjusts the center of gravity to prevent slipping, is limited. The aforementioned studies primarily focused on the dynamics of slipping motion, without developing controllers to investigate the effectiveness of dynamic models. WMR considering slip are multivariable nonlinear systems. Various uncertainties exist in dynamics due to external disturbances and nonlinear friction, making it challenging to establish accurate mathematical models. Wang et al. [10] introduced slip parameters in mobile robot dynamics and utilized adaptive control techniques to compensate for errors in longitudinal slip. Nguyena et al. [11] established an online updating rate of Gaussian wavelet networks in controllers to approximate unknown nonlinear functions dynamically. The aforementioned studies treated slipping as a disturbance without addressing it specifically. Therefore, this paper designs a sliding mode observer based on sensor feedback information such as the robot's reference trajectory and drive wheel speeds to observe the slipping parameters of the left and right wheels.

As research into trajectory tracking control for wheeled mobile robots advances, various soft computing methods

Manuscript received April 25, 2024; revised September 10, 2024.

This work was supported by the National Natural Science Foundation of China (61772247), The Industry-Academia-Research Cooperation Projects of Jiangsu Province (BY2022651), The Key Foundation projects of Lishui(2023LTH03). Discipline Construction Project of Lishui University (Discipline Fund Name: Mechanical Engineering)

Linghong Zhu is an associate professor at School of Intelligent Manufacturing, Lishui Vocational and Technical College, Lishui 323000, P. R. China (e-mail: 715703595@qq.com).

Xiaochen Huang is a postgraduate student in the School of Mechanical Engineering at Zhejiang Sci-Tech University, Hangzhou 310018, P. R. China (email: hxc1249006389@163.com).

Xiaoming Wu is a professor at School of Intelligent Manufacturing, Lishui Vocational and Technical College, Lishui 323000, P. R. China (e-mail: 668918@qq.com).

Rui Chen is a postgraduate student in the School of Mechanical Engineering at Zhejiang Sci-Tech University, Hangzhou 310018, P. R. China (email: cr1716707642@126.com).

Dajian Yi is a postgraduate student in the School of Mechanical Engineering at Zhejiang Sci-Tech University, Hangzhou 310018, P. R. China (email: ydj1176540684@163.com).

Wenhui Zhang is a professor at Nanjing Xiaozhuang University, Nanjing 211171, P. R. China (corresponding author to provide phone: +8618268906955; e-mail: hit_zwh@126.com)

have been applied [12-17]. In recent years, controllers based on neural networks have been widely used in the field of robotics [18-21]. Hoang et al. [22] proposed a neural network adaptive controller based on online weight updating rules to manage uncertainties caused by wheel slippage and external forces, aiming to achieve desired tracking performance. However, in highly uncertain dynamic systems, the adaptive updating of neural network weights, due to the large number of neurons, requires extended periods of observation and learning, making it unsuitable for online control. Wavelet Neural Networks (WNNs) integrate wavelets with neural networks. Wavelet networks possess the ability to analyze non-stationary signals to uncover local details, with characteristics such as simple structure, fast learning speed, higher efficiency compared to traditional neural networks, and easier training [23, 24]. Nevertheless, there exists a significant relationship between the approximation of mobile robot dynamics and approximation errors, leading to performance degradation of the controller. Therefore, to minimize the impact of approximation errors to a predetermined level, this paper proposes an H∞ controller.

In summary, this paper proposes a mobile robot control scheme that integrates fuzzy logic, Waveform Neural Network (WNN), sliding mode observer, and H∞ control. The scheme aims to achieve high-precision position tracking under wheel slip conditions, with capabilities of rapid learning, fast convergence, and compensation for structured and unstructured uncertainties. Additionally, Lyapunov theory is employed to demonstrate the asymptotic stability of the closed-loop system. The main contributions of this study are as follows:

(i) A novel FWNN is designed by integrating Takagi-Sugeno-Kang (TSK) fuzzy system and WNN. By combining and defuzzifying two types of output signals at the output layer, the overall network output is optimized, thereby enhancing the network's generalization ability.

(ii) A sliding mode observer is designed to online estimate parameters related to wheel slip, based on the correlation between vehicle posture and reference trajectory, and the relationship between left and right wheel speeds. To address chattering in sliding mode variable structure, a novel sinusoidal saturation function is designed to eliminate oscillations.

(iii) A robust controller is designed using H∞ theory to address approximation errors of neural network approximations of unknown robot dynamics and disturbances introduced by interference signals. The controller aims to bound all parameter errors and control signals, ensuring that error signals decay within specified boundaries.

II. Kinematic and Dynamic Modeling of WMR

Robotic kinematic modeling serves as the foundation for robotic motion control, with the accuracy of the model directly influencing control precision. However, solely tracking trajectories at the kinematic level often falls short of achieving the desired performance metrics. Therefore, this paper considers integrating kinematics and dynamics to establish functional relationships between torque and velocity [25-27].

In ideal circumstances, the Lagrangian formulation of dynamics equations for WMRs is typically represented as:

$$M(q)\ddot{q}+V(q,\dot{q})\dot{q}+G(q)+\tau_d+A^T(q)\lambda=T(q)\tau \quad (1)$$

Where: $M(q)$ represents the inertia matrix, $V(q,\dot{q})$ denotes the Coriolis matrix, $G(q)$ stands for the gravitational term, $T(q)$ signifies the transformation matrix, $A^T(q)$ is the matrix associated with constraints, τ represents the torque term, and λ denotes the Lagrangian operator.

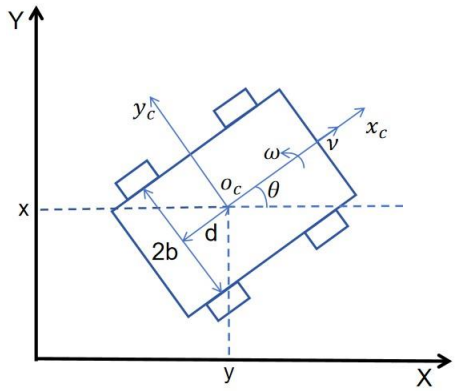

Fig. 1 WMR movement diagram

The schematic diagram in Fig. 1 illustrates a WMR with non-coincident geometric center and center of mass; XOY represents the inertial coordinate system, while $x_c o_c y_c$ denotes the robot coordinate system. $q=[x,y,\theta]^T$ represents the position and orientation angle of the robot in the inertial coordinate system.

The transformation of the velocity of the robot's center of mass from the inertial coordinate system to the robot coordinate system can be calculated as follows:

$$\dot{q}=\begin{bmatrix}\dot{x}\\ \dot{y}\\ \dot{\theta}\end{bmatrix}=\begin{bmatrix}\cos\theta & -\sin\theta & 0\\ \sin\theta & \cos\theta & 0\\ 0 & 0 & 1\end{bmatrix}\begin{bmatrix}v_x\\ v_y\\ w\end{bmatrix} \quad (2)$$

By combining equations (1) and (2), the kinematic model of the robot in the inertial coordinate system can be obtained:

$$\begin{bmatrix}\dot{x}\\ \dot{y}\\ \dot{\theta}\end{bmatrix}=\begin{bmatrix}\frac{r\cos\theta}{2} & \frac{r\cos\theta}{2}\\ \frac{r\sin\theta}{2} & \frac{r\sin\theta}{2}\\ -\frac{r}{d} & \frac{r}{d}\end{bmatrix}\begin{bmatrix}\omega_l\\ \omega_r\end{bmatrix} \quad (3)$$

ω_l and ω_r denote the angular velocities of the left and right wheels. For simplification, let the transformation matrix $\Gamma(\theta)$ be defined as follows:

$$\Gamma(\theta)=\begin{bmatrix}\frac{r\cos\theta}{2} & \frac{r\cos\theta}{2}\\ \frac{r\cos\theta}{2} & \frac{r\cos\theta}{2}\\ -\frac{r}{d} & \frac{r}{d}\end{bmatrix} \quad (4)$$

When the robot experiences wheel slippage during motion, define the slip ratio as i:

$$i=\frac{r\omega-v'}{r\omega} \quad (5)$$

In equation (5), v' represents the actual velocity of the wheel relative to the ground when wheel slippage occurs. When i = 1, it means the wheel is completely slipping and

spinning freely without traction, resulting in the robot being stationary relative to the ground. At this point, the robot is in a completely uncontrollable state, and studying this scenario is meaningless. Therefore, the range of the slip ratio is defined as $0 \le i < 1$.

The velocity of the wheel relative to the ground when the wheel is slipping is:

$$v' = r\omega(1-i) \tag{6}$$

Therefore, the kinematic model of the robot under slip conditions is:

$$\begin{bmatrix} \omega_l \\ \omega_r \end{bmatrix} = \begin{bmatrix} \frac{1}{1-i_l} & 0 \\ 0 & \frac{1}{1-i_r} \end{bmatrix} \begin{bmatrix} \bar{\omega}_l \\ \bar{\omega}_r \end{bmatrix} \tag{7}$$

Obtained from equations (4) and (7)

$$\bar{\Gamma}(\theta) = \Gamma(\theta) \begin{bmatrix} \frac{1}{1-i_l} & 0 \\ 0 & \frac{1}{1-i_r} \end{bmatrix} \tag{8}$$

$\bar{v} = \begin{bmatrix} r\bar{\omega}_l & r\bar{\omega}_r \end{bmatrix}^T$ is the current speed of the wheel compared to the ground. By substituting equations (4) and (8) into formula (3), the kinematic model of WMR longitudinal slip is obtained as follows:

$$\dot{q} = \bar{\Gamma}(\theta)\bar{v} \tag{9}$$

Substituting equation (9) into equation (1), we obtain the dynamic model of longitudinal slip for a WMR.

$$\bar{M}(\bar{v})\dot{\bar{v}} + \bar{C}(\bar{v})\bar{v} + \bar{\tau}_d = \bar{T}(\bar{v})\tau \tag{10}$$

In equation (10), $\bar{M}(\bar{v}) = \bar{\Gamma}^T M \bar{\Gamma}, \bar{C}(\bar{v}) = \bar{\Gamma}^T (M\dot{\bar{\Gamma}} + C\bar{\Gamma})$ $\bar{\tau}_d = \bar{\Gamma}^T \tau_d$, $\bar{T}(\bar{v}) = \bar{\Gamma}^T B$ .Moreover, for any n-dimensional vector, the following property holds:

$$x^T(\bar{M}(\bar{v}) - 2\bar{C}(\bar{v}))x = 0 \tag{11}$$

III. Observer Design Based on Sliding Mode

Design the control system as illustrated in Fig. 2

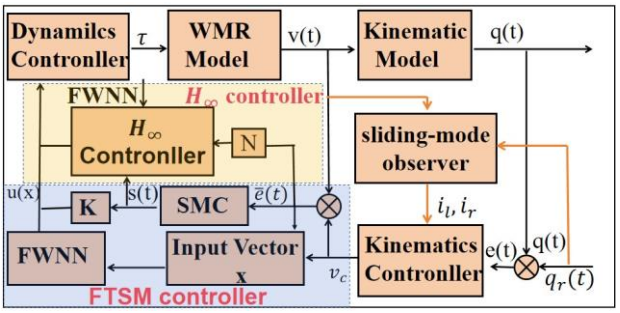

Fig. 2 Control system framework

A. Observer design based on sliding mode

The actual velocity of the mobile robot can also be represented as follows:

$$v = \frac{r\omega_l(1-i_l) + r\omega_r(1-i_r)}{2} \tag{12}$$

It can be obtained by formula (3) and formula (12)

$$\dot{\theta} = \frac{2v - 2r\omega_l(1-i_l)}{l} = -\frac{2v + 2r\omega_r(1-i_r)}{l} \tag{13}$$

$\hat{\theta}_1, \dot{\hat{\theta}}_1, \dot{\theta}_1$, and $\hat{\theta}_2, \dot{\hat{\theta}}_2, \dot{\theta}_2$, are both introduced as virtual directional variables for the robot, where $\dot{\theta}_1 = \dot{\theta}_2 = \dot{\theta}$. Express the virtual variables $\dot{\theta}_1$ and $\dot{\theta}_2$ as follows:

$$\begin{aligned} \dot{\theta}_1 &= \frac{2v - 2r\omega_l(1-i_l)}{l} \\ \dot{\theta}_2 &= -\frac{2v + 2r\omega_r(1-i_r)}{l} \end{aligned} \tag{14}$$

The sliding mode observer is designed according to formula (14) as follows:

$$\begin{aligned} \dot{\theta}_1 &= \frac{2v}{l} + L_1 \operatorname{sgn}(\theta - \hat{\theta}_1) + L(\theta - \hat{\theta}_1) \\ \dot{\theta}_2 &= -\frac{2v}{l} + L_2 \operatorname{sgn}(\theta - \hat{\theta}_2) + L(\theta - \hat{\theta}_2) \end{aligned} \tag{15}$$

In the equation, the parameters L , L_1 and L_2 represent the gains of the sliding mode observer, both of which are positive numbers.

Define the differential equations for observation errors as $\tilde{\dot{\theta}}_1 = \dot{\theta}_1 - \dot{\hat{\theta}}_1$, $\tilde{\dot{\theta}}_2 = \dot{\theta}_2 - \dot{\hat{\theta}}_2$. By combining the above equations (14) and (15), the following equation is obtained:

$$\begin{aligned} \tilde{\dot{\theta}}_1 &= -\frac{2r\omega_l(1-i_l)}{l} - L_1 \operatorname{sgn}(\theta - \hat{\theta}_1) - L(\theta - \hat{\theta}_1) \\ \tilde{\dot{\theta}}_2 &= \frac{2r\omega_r(1-i_r)}{l} - L_2 \operatorname{sgn}(\theta - \hat{\theta}_2) - L(\theta - \hat{\theta}_2) \end{aligned} \tag{16}$$

Given the appropriate selection of sliding mode observer gains, observation errors will converge to the sliding mode surface within a valid time frame. Thus, it follows from the above equation:

$$\begin{aligned} -\frac{2r\omega_l(1-i_l)}{l} - L_1 \operatorname{sgn}(\theta - \hat{\theta}_1) - L(\theta - \hat{\theta}_1) \approx 0 \\ \frac{2r\omega_r(1-i_r)}{l} - L_2 \operatorname{sgn}(\theta - \hat{\theta}_2) - L(\theta - \hat{\theta}_2) \approx 0 \end{aligned} \tag{17}$$

If the angular velocities of the two drive wheels of the mobile robot are measurable, the reference trajectory of the mobile robot is given, and the gains of the sliding mode observer are known, the estimated values of the sliding parameters can be expressed as follows:

$$\begin{aligned} \hat{i}_l &= 1 + \frac{l\left[L_1 \operatorname{sgn}(\theta - \hat{\theta}_1) - L(\theta - \hat{\theta}_1)\right]}{2r\omega_l} \\ \hat{i}_r &= 1 - \frac{l\left[L_2 \operatorname{sgn}(\theta - \hat{\theta}_2) - L(\theta - \hat{\theta}_2)\right]}{2r\omega_r} \end{aligned} \tag{18}$$

The presence of the sign function $\operatorname{sgn}(x)$ in the sliding mode observer leads to high-frequency switching of the control signal, causing discontinuities in control and resulting in chattering phenomena. Chattering severely affects control accuracy, increases energy consumption, and can even render the control system inoperable. In this study, a sine saturation function is proposed to replace the sign function $\operatorname{sgn}(x)$. The expression of the new sine saturation function is as follows:

$$sat(s, \Delta) = \begin{cases} \operatorname{sgn}(s) & |s| \ge \Delta \\ \sin(\lambda s) & |s| < \Delta \end{cases} \tag{19}$$

Here, Δ represents the thickness of the boundary layer, and $\lambda = 2/\pi\Delta$. With this approach, switch control is utilized outside the saturation layer, while linear control is employed within the saturation layer. This ensures convergence speed

while reducing chattering caused by high-frequency switching.

B. Stability analysis

The switching function of the sliding mode observer is defined as:

$$\begin{aligned} s_1 &= \theta - \hat{\theta}_1 \\ s_2 &= \theta - \hat{\theta}_2 \end{aligned} \tag{20}$$

Construct the Lyapunov function based on s_1 as follows:

$$V_1 = \frac{1}{2} s_1^2 \tag{21}$$

Differentiating the above equation and combining it with formulas (14) and (15), we obtain:

$$\dot{V}_1 = s_1 \cdot \dot{s}_1 = -\frac{2r\omega_l(1-i_l)}{l} \cdot s_1 - L_1 sat(\theta - \hat{\theta}_1) \cdot s_1 - L s_1^2 \tag{22}$$

When the sliding mode gain L is chosen as a relatively small positive number, the following relationship is derived:

$$\dot{V}_1 < \frac{2r}{l} |\omega_l(1-i_l)||s_1| - L_1 |s_1| \le 0 \tag{23}$$

To ensure that the state error converges to zero in a finite time, the sliding mode gain L_1 satisfies the following relationship:

$$L_1 \ge \frac{2r}{l} |\omega_l|^+ |1 - \mathrm{i}_l|^+ \tag{24}$$

Similarly, constructing the Lyapunov function based on s_2 yields the following:

$$V_2 = \frac{1}{2} s_2^2 \tag{25}$$

Differentiating the above equation and combining it with formulas (14) and (15), we obtain:

$$\begin{aligned} \dot{V}_2 &= s_2 \cdot \dot{s}_2 \\ &= -\frac{2r\omega_r(1-i_r)}{l} \cdot s_2 - L_2 sat(\theta - \hat{\theta}_2) \cdot s_2 - L {s_2}^2 \\ &< \frac{2r}{l} |\omega_r(1-i_r)||s_2| - L_2 |s_2| \le 0 \end{aligned} \tag{26}$$

To ensure that the state error converges to zero in a finite time, the sliding mode gain L_2 satisfies the following relationship:

$$L_2 \ge \frac{2r}{l} |\omega_r|^+ |1 - \mathrm{i}_r|^+ \tag{27}$$

IV. 4 Controller design based on FWNN

A. 4.1 Controller design based on dynamic models

Considering the significant disparity between the velocity of the kinematic portion and the actual velocity of a WMR under slipping conditions, relying solely on the velocity of a kinematic controller may not achieve the desired control effectiveness. Therefore, introducing kinematic auxiliary control into dynamic control is necessary to design the controller.

Given the reference trajectory $q_r(t) = (x_r, y_r, \theta_r)^T$ and the actual motion trajectory $q(t) = (x, y, \theta)^T$. Tracking error can be expressed as:

$$e(t) = \begin{bmatrix} \cos\theta & \sin\theta & 0 \\ -\sin\theta & \cos\theta & 0 \\ 0 & 0 & 1 \end{bmatrix} \begin{bmatrix} x_r - x \\ y_r - y \\ \theta_r - \theta \end{bmatrix} \tag{28}$$

Taking the derivative of $e(t)$ gives:

$$\dot{e}(t) = \begin{bmatrix} v_r \cos\theta_r - v + x_e\dot{\theta} \\ v_r \sin\theta + x_e\dot{\theta} \\ w_r - \dot{\theta} \end{bmatrix} \tag{29}$$

The auxiliary speed controller is designed:

$$\begin{bmatrix} v_c \\ w_c \end{bmatrix} = \begin{bmatrix} v_r \cos\theta_e + k_1 x_e \\ w_r + k_2 v_r y_e + k_3 v_r \sin\theta_e \end{bmatrix} \tag{30}$$

$\begin{bmatrix} v_r & w_r \end{bmatrix}^T$ represents the desired velocity, v_c, w_c represents the linear velocity and angular velocity of the mobile robot at a point. In equation (30), k_1, k_2, k_3 are all positive numbers. Construct the Lyapunov function as follows:

$$V_2 = \frac{1}{2} e_1^2 + \frac{1}{2} e_2^2 + \frac{1}{k_2}(1 - \cos e_3) \tag{31}$$

Take the derivative of V_2:

$$\dot{V}_2 = e_1\dot{e}_1 + e_2\dot{e}_2 + \frac{1}{k_2}\dot{e}_3 \sin e_3 \tag{32}$$

Substituting equation (30) into the above expression, we obtain:

$$\dot{V}_2 = -k_1 e_1^2 - \frac{k_3}{k_2} \sin^2 e_3 \tag{33}$$

The above proof shows that $V_2 \ge 0$ and $\dot{V}_2 \le 0$. Therefore, the system is asymptotically stable.

B. Controller design based on FWNN

The linear and angular velocity of the mobile robot at a point is converted to the speed of the wheel relative to the ground.

$$\begin{bmatrix} \bar{\boldsymbol{v}}_{\boldsymbol{l}} \\ \bar{\boldsymbol{v}}_{\boldsymbol{r}} \end{bmatrix} = \begin{bmatrix} 1 & -\boldsymbol{b} \\ 1 & \boldsymbol{b} \end{bmatrix} \begin{bmatrix} \boldsymbol{v}_{\boldsymbol{c}} \\ \boldsymbol{w}_{\boldsymbol{c}} \end{bmatrix} \tag{34}$$

$v_d = \begin{bmatrix} \bar{v}_l & \bar{v}_r \end{bmatrix}$, $\bar{v}$ represents the actual velocity of the wheel relative to the ground. To track the desired velocity, we introduce the velocity tracking error:

$$\bar{e}(t) = \bar{v} - v_d \tag{35}$$

Define the sliding mode surface as:

$$s = \dot{\bar{e}} + \Lambda\bar{e} \tag{36}$$

The dynamics of WMR can be expressed as:

$$\bar{M}\dot{s} = -\bar{C}s - \bar{\mathrm{T}}\tau + u(x) + \bar{\tau}_d \tag{37}$$

The function $u(x) = \bar{M}(v)(\dot{\bar{v}} + \Lambda\dot{\bar{e}}) + \bar{C}(v)(\bar{v} + \Lambda\bar{e})$ is termed as the non-linear function representing the WMR slippage. We choose the input vector $x = \begin{bmatrix} \bar{e} & \dot{\bar{e}} & v_d & \dot{v}_d \end{bmatrix}$. Hence, it can be observed that the non-linear function of WMR exhibits both structured and unstructured uncertainties. To address this uncertain model, we employ a fuzzy wavelet network for estimating this function.

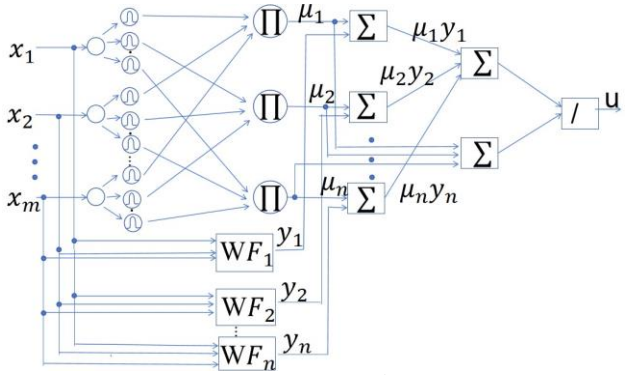

Fig 3 The structure of FWNN

As illustrated in Fig 3, FWNN proposed in this section combines the WNN with the TSK fuzzy system.

First Layer: Input Layer. Vector $x=\left[\bar{e} \quad \dot{\bar{e}} \quad v_d \quad \dot{v}_d\right]$ serves as the input.

Second Layer: Membership Layer. Each node in this layer corresponds to a fuzzy membership function.

$$\Psi(x_i)=\bar{e}^{-a_j^2(x_i-b_{ji})^2}, i=1,...,m;\ j=1,...,n, \tag{38}$$

The third layer: Fuzzy rule layer.

$$\begin{aligned}&\mu_j(x_i)=\prod_{i=1}^{m}\Psi_j(x_i), y_j=W_j\psi_j(x_i),\\ &i=1,...,m,\ j=1,...,n,\\ &\psi_j(x_i)=\left[1-a_{ji}^2(x_i-b_{ji})^2\right]\bar{e}^{-a_{ji}^2(x_i-b_{ji})^2}\end{aligned} \tag{39}$$

The fourth layer: Output layer. The output signals from the previous layer are multiplied by the signals outputted from the WNN and then defuzzified.

$$u=\sum_{j=1}^{n}\mu_j(x)y_j/\sum_{j=1}^{n}\mu_j(x) \tag{40}$$

Then u can be expressed as:

$$\begin{aligned}&u(x,a,b,W)=\left[u_1,u_2,...,u_n\right]^T=W^T\mu(x,a,b)\\ &a=\left[a_1,a_2,...,a_n\right]^T\in R^{Nm}\\ &b=\left[b_1,b_2,...,b_n\right]^T\in R^{Nm}\\ &\mu(x,a,b)=\left[\mu_1,\mu_2,...,\mu_n\right]^T\\ &W=\left[w_1,w_2,...,w_n\right]^T\in R^{nN}\end{aligned} \tag{41}$$

FWNN has a strong approximate error analysis, then there is a nonlinear dynamic u(x) with optimal parameters:

$$u(x)=W^{*T}\mu^*(x^*,a^*,b^*)+u_0(x) \tag{42}$$

W^*, a^*, b^* are the optimal parameters of W,a,b respectively, and $u(x)$ is the minimum approximation error vector. The approximate design of the output FWNN is:

$$\begin{aligned}&\hat{u}=\hat{W}^T\hat{\mu}(x,\hat{a},\hat{b})\\ &\tilde{u}=u-\hat{u}=W^{*T}\mu^*-\hat{W}^T\hat{\mu}+u_0\end{aligned} \tag{43}$$

Define the parameter error: $\tilde{W}=W^*-\hat{W};\tilde{a}=a^*-\hat{a};$ $\tilde{b}=b^*-\hat{b};\tilde{\mu}=\mu^*-\hat{\mu}$, equation (43) can be written as:

$$\tilde{u}=W^{*T}\tilde{\mu}+\tilde{W}^T\hat{\mu}+u_0 \tag{44}$$

$\tilde{u}$ can be expanded as a Taylor series:

$$\begin{aligned}\tilde{\mu}=&\left[\frac{\partial\mu_1}{\partial a},\frac{\partial\mu_2}{\partial a},...,\frac{\partial\mu_N}{\partial a}\right]_{a=\hat{a}}\tilde{a}\\ &+\left[\frac{\partial\mu_1}{\partial b},\frac{\partial\mu_2}{\partial b},...,\frac{\partial\mu_N}{\partial b}\right]_{b=\hat{b}}\tilde{b}+H(\tilde{a},\tilde{b})\end{aligned} \tag{45}$$

$$\mathrm{A}^T=\left[\frac{\partial\mu_1}{\partial a},\frac{\partial\mu_2}{\partial a},...,\frac{\partial\mu_N}{\partial a}\right]_{a=\hat{a}}\in R^{\mathrm{N}\times(\mathrm{Nm})}$$

$$\mathrm{B}^T=\left[\frac{\partial\mu_1}{\partial b},\frac{\partial\mu_2}{\partial b},...,\frac{\partial\mu_N}{\partial b}\right]_{a=\hat{a}}\in R^{N\times(Nm)}$$

Then the above formula can be written as:

$$\tilde{u}=A^T\tilde{a}+B^T\tilde{b}+H(\tilde{a},\tilde{b}) \tag{46}$$

Substitute equation (46) into equation (43) to get:

$$\begin{aligned}\tilde{u}=&\tilde{W}^T\left[\hat{u}+A^T(a^*-\hat{a})+B^T(b^*-\hat{b})\right]\\ &+\hat{W}(A^T\tilde{a}+B^T\tilde{b})+W^{*T}H(\tilde{a},\tilde{b})+u_0\\ \tilde{u}=&\tilde{W}^T\left(\hat{u}-A^T\hat{a}-B^T\hat{b}\right)+\hat{W}^T\left(A^T\tilde{a}+B^T\tilde{b}\right)\\ &+\omega'(x,a,b)\\ \omega'(x,a,b)=&\hat{W}^T\left(A^T\tilde{a}+B^T\tilde{b}\right)+W^{*T}H(\tilde{a},\tilde{b})+u_0\end{aligned} \tag{47}$$

Let

$$\omega(x,a,b)=\hat{W}^T\left(A^T\tilde{a}+B^T\tilde{b}\right)+W^{*T}H(\tilde{a},\tilde{b})+u_0+\bar{\tau}_d \tag{48}$$

Then the dynamics of WMR can be described as:

$$\begin{aligned}\bar{M}\dot{s}=&-\bar{C}s-\bar{T}(\bar{v})\tau+\hat{W}^T\mu(x,\hat{a},\hat{b})\\ &+\tilde{W}^T(\hat{\mu}-A\hat{a}-B\hat{b})+\hat{W}^TA\tilde{a}+\hat{W}^TB\tilde{b}+\omega\end{aligned} \tag{49}$$

C. *Design of FWNN controller based on H_∞*

Introducing approximation errors in the dynamics of unknown robots through FWNN approximation can lead to a decrease in the performance of controllers. Therefore, to mitigate the impact of approximation errors to a predetermined level, this paper proposes an H_∞ controller-based approach.

The control goal is to design the controller so that the closed-loop system meets the following requirements:

1. If the perturbation term has a finite energy $\omega\in L_2[0,t]$, for all t≥0, then all errors in the FWNN parameters, as well as the control signal, are bounded and e(t) converges to 0.

2. Under the specified attenuation level $\chi<0$, the system must meet the $H\infty$ tracking performance requirements as follows:

$$\begin{aligned}\int_0^T\bar{e}^TZ\bar{e}dt\le&s^T(0)M_0s(0)+\bar{e}^T(0)N\bar{e}(0)\\ &+tr(\tilde{W}^T(0)\Theta_w^{-1}\tilde{W}(0))+\tilde{a}^T(0)\Theta_a^{-1}\tilde{a}(0)\\ &+\tilde{b}^T(0)\Theta_b^{-1}\tilde{b}(0)+\chi^2\int_0^T\|\omega\|^2dt\end{aligned} \tag{50}$$

Here, $Z=Z^T$, and Z is a positive definite matrix where $T\in(0,\infty)$.

According to formula (49), we assume that the selection control law is:

$$\tau=\bar{\mathrm{T}}^{-1}(v)(\hat{W}^T\hat{u}+K\,\mathrm{sgn}(s)+N\bar{e}+\frac{s}{2\chi^2}) \tag{51}$$

K is a positive definite matrix, and if $Z=2N\Lambda_1$.then the updating rule of parameters of FWNN is as follows:

$$\begin{aligned}\dot{\hat{W}} &= \Theta_W(\hat{\mu} - A\hat{a} - B\hat{b})s^T \\ \dot{\hat{a}} &= \Theta_a A^T \hat{W} s \\ \dot{\hat{b}} &= \Theta_b B^T \hat{W} s\end{aligned} \tag{52}$$

Here, $\Theta_W \in \mathrm{R}^{N\times N}, \Theta_a \in \mathrm{R}^{N\times N}, \Theta_b \in \mathrm{R}^{N\times N}$ are all positive definite matrices. Then all FWNN parameter errors and control signals are bounded, and the tracking error $\bar{e} \to 0$ satisfies the H_∞ tracking performance guarantee given by equation (52).

D. 4.4 Stability analysis based on Lyapunov

Select the Lyapunov function as:

$$\begin{aligned}V &= \frac{1}{2}s^T \bar{M} s + \frac{1}{2}\bar{e}^T P \bar{e} + \frac{1}{2}tr(\tilde{W}^T \Theta_W^{-1} \tilde{W}) \\ &+ \frac{1}{2}\tilde{a}^T \Theta_a^{-1} \tilde{a} + \frac{1}{2}\tilde{b}^T \Theta_b^{-1} \tilde{b}\end{aligned} \tag{53}$$

Take the derivative of t on both sides, substituting in the control law (51), and using $s^T s = \|s\|^2$, properties (11), and updating rules of the parameters of FWNN $\dot{\tilde{W}} = -\dot{\hat{W}}, \dot{\tilde{a}} = -\dot{\hat{a}}, \dot{\tilde{b}} = -\dot{\hat{b}}$.

$$\begin{aligned}\dot{V} &= s^T M \dot{s} + \frac{1}{2}s^T \dot{M} s + e^T N \dot{e} + tr(\tilde{W}^T \Theta_w^{-1} \dot{\tilde{W}}) \\ &+ \tilde{a}^T \Theta_a^{-1} \dot{\tilde{a}} + \tilde{b}^T \Theta_b^{-1} \dot{\tilde{b}} \\ &= \frac{1}{2}s^T (\dot{M} - 2V_m)\ s - s^T K \operatorname{sgn}(s) - s^T N e \\ &- \frac{s^T s}{2\chi^2} + s^T \tilde{W}(\hat{u} - A\hat{a} - B\hat{b}) + s^T \hat{W}^T A\tilde{a} \\ &+ s^T \hat{W}^T B\tilde{b} + s^T \omega + e^T N \dot{e} + tr(\tilde{W}^T \Theta_w^{-1} \dot{\tilde{W}}) \\ &+ \tilde{a}^T \Theta_a^{-1} \dot{\tilde{a}} + \tilde{b}^T \Theta_b^{-1} \dot{\tilde{b}} \\ &\le -s^T N e - \left(\frac{\|s\|^2}{2\rho^2} - \|s\|\|\omega\| + \frac{1}{2}\chi^2 \|\omega\|^2 \right) \\ &+ \frac{1}{2}\chi^2 \|\omega\|^2 + e^T N \dot{e} + s^T \hat{W}^T A\tilde{a} + \\ &s^T \tilde{W}(\hat{u} - A\hat{a} - B\hat{b}) + s^T \hat{W}^T B\tilde{b} \\ &+ tr(\tilde{W}^T \Theta_w^{-1} \dot{\tilde{W}}) + \tilde{a}^T \Theta_a^{-1} \dot{\tilde{a}} + \tilde{b}^T \Theta_b^{-1} \dot{\tilde{b}} \\ &\le -s^T N e + \frac{1}{2}\chi^2 \|\omega\|^2 + e^T N \dot{e} \\ &+ s^T \tilde{W}(\hat{u} - A\hat{a} - B\hat{b}) + s^T \tilde{W}^T A\tilde{a} + s^T \hat{W}^T B\tilde{b} \\ &+ tr(\tilde{W}^T \Theta_w^{-1} \dot{\tilde{W}}) + \tilde{a}^T \Theta_a^{-1} \dot{\tilde{a}} + \tilde{b}^T \Theta_b^{-1} \dot{\tilde{b}}\end{aligned} \tag{54}$$

Replace equation (36) with $\dot{\bar{e}} = s - \Lambda \bar{e}$ to get:

$$\dot{V} \le -s^T N \bar{e} + \frac{1}{2}\chi^2 \|\omega\| + \bar{e}^T N s - \bar{e}^T N \Lambda \bar{e} \tag{55}$$

Substitute $Z = 2N\Lambda_1$ into the above equation.

$$\dot{V} \le \frac{1}{2}\chi^2 \|\omega\|^2 - \frac{1}{2}\bar{e}^T Z \bar{e} \tag{56}$$

Integrating the above formula from 0 to T yields:

$$V(T) - V(0) \le \frac{1}{2}\chi^2 \int_0^T \|\omega\|^2 dt - \frac{1}{2}\int_0^T \bar{e}^T Z \bar{e} dt \tag{57}$$

Considering $V(T) \ge 0$, and using the value of V(0) in equation (42), the H_∞ tracking performance required by the controller can be obtained as follows:

$$\begin{aligned}\int_0^T \bar{e}^T Z \bar{e} dt &\le s^T(0) M_0 s(0) + \bar{e}^T(0) N \bar{e}(0) \\ &+ tr(\tilde{W}^T(0)\Theta_w^{-1}\tilde{W}(0)) + \tilde{a}^T(0)\Theta_a^{-1}\tilde{a}(0) \\ &+ \tilde{b}^T(0)\Theta_b^{-1}\tilde{b}(0) + \chi^2 \int_0^T \|\omega\|^2 dt\end{aligned} \tag{58}$$

The inequality (57) is rewritten as the integral from 0 to t in order to establish the bound-ability of the parameter error and control signal of FWNN.

$$V(t) \le V(0) + \frac{1}{2}\chi^2 \int_0^t \|N\|^2 dt \le \frac{1}{2}\chi^2 \int_0^t \|N\|^2 dt \tag{59}$$

Since, for all $t \ge 0, \omega \in L_2[0,t]$, we derive $V(t) < \infty$. This establishes boundness for all error signals $\bar{e}, s, \tilde{W}, \tilde{a}, \tilde{b}$. Thus, the boundedness of $\bar{v}, W, a, b, \hat{W}, \hat{a}, \hat{b}$ and the control signal τ is proved. In order to obtain asymptotic stability of the system, we choose the following Lyapunov function:

$$V = V_1 + V_2 = \frac{1}{2}s^T M s + \frac{1}{2}\bar{e}^T N \bar{e} \tag{60}$$

Take the derivative of t on both sides, substitute the control law (40), and use $s^T s = \|s\|^2$, we get

$$\begin{aligned}\dot{V} &= -s^T K \operatorname{sgn}(s) - s^T N e - \frac{\|s\|^2}{2\chi^2} + \bar{e}^T N \dot{\bar{e}} \\ &+ s^T \left[\tilde{W}^T(\hat{u} - A\hat{a} - B\hat{b}) + \tilde{W}^T A\tilde{a} + \tilde{W}^T B\tilde{b} + \omega \right] \\ &\le -\lambda_{\min}(K)\|s\| - s^T N e + \bar{e}^T N s - \bar{e}^T N \Lambda \bar{e} \\ &+ \|s\| \left\| \tilde{W}^T(\hat{u} - A\hat{a} - B\hat{b}) + \hat{W}^T A\tilde{a} + \hat{W}^T B\tilde{b} + \omega \right\| \\ &\le -\lambda_{\min}(K)\|s\| + \|s\| \left\| \tilde{W}^T(\hat{u} - A\hat{a} - B\hat{b}) \right. \\ &\left. + \hat{W}^T A\tilde{a} + \hat{W}^T B\tilde{b} + \omega \right\|\end{aligned} \tag{61}$$

Where $\lambda_{\min}$ is the least singular value of the matrix K. Since the tracking error $\bar{e}$, $\dot{\bar{e}}$ is bounded, and the expected velocity v_d is also bounded, a boundedness of the input vector x is established. Since, any Gaussian function $\phi(x)$ is bounded as $0 < \|\phi(x)\| \le 1$; Therefore, the boundedness of $\hat{u}$ and matrices a and b is obtained by using the estimated boundedness of the WNN parameter $\hat{W}, \hat{a}, \hat{b}$ and the input vector x. Assuming boundedness of the perturbation term ω, we get

$$\begin{aligned}&\left\| \tilde{W}^T(\hat{u} - A\hat{a} - B\hat{b}) + \hat{W}^T A\tilde{a} + \hat{W}^T B\tilde{b} + \omega \right\| \\ &\le \left\| \tilde{W}^T(\hat{u} - A\hat{a} - B\hat{b}) \right\| + \left\| \hat{W}^T A\tilde{a} \right\| + \left\| \hat{W}^T B\tilde{a} \right\| + \|\omega\| \\ &\le \left\| \tilde{W} \right\|_F \left\| \hat{u} - A\hat{a} - B\hat{b} \right\| + \left\| \hat{W} \right\|_F \|A\|_F \|\tilde{a}\| + \left\| \hat{W} \right\|_F \|B\|_F \left\| \tilde{b} \right\| + \|\omega\| \\ &\le K_{m1} + K_{m2} + K_{m3} + K_{m4} = K_M\end{aligned} \tag{62}$$

Where $\|.\|_F$ represents the Frobenius norm. If the gain matrix K is chosen so that $\lambda_{\min} > K_M$, s will asymptotically converge to zero according to the two-point requirement of the H_∞ closed-loop system. Using the definition of sliding surface, it can be deduced that the tracking error along the sliding surface asymptotically converges to zero.

V. Simulation Experiment

The physical model of the mobile robot under wheel slip condition is shown in the figure, and its dynamic model

equation (10) is used as the numerical simulation experimental object to verify the proposed algorithm.

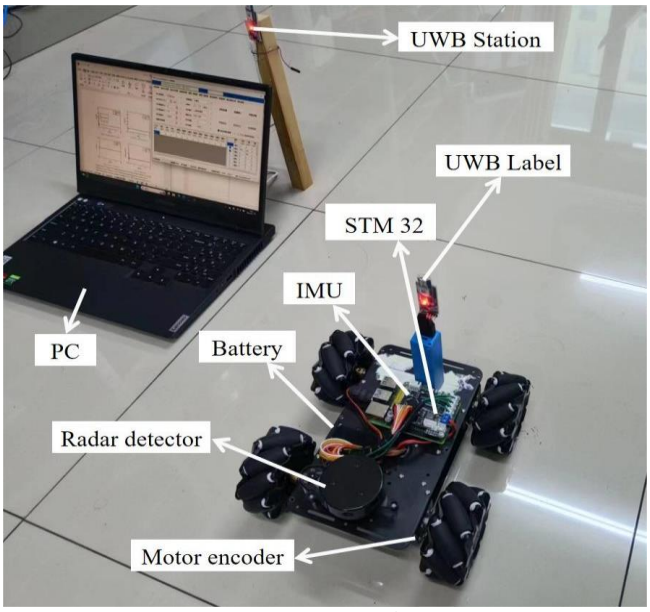

Fig. 4 WMR platform

$$\bar{M}\dot{\bar{v}} + \bar{C}\bar{v} + \bar{\tau}_d = \bar{T}\tau$$

$$\bar{M} = \begin{bmatrix} \frac{r^2}{4b^2}(mb^2 + I) + I_\omega & \frac{r^2}{4b^2}(mb^2 - I) \\ \frac{r^2}{4b^2}(mb^2 - I) & \frac{r^2}{4b^2}(mb^2 + I) + I_\omega \end{bmatrix} \tag{63}$$

$$\bar{C} = \begin{bmatrix} 0 & \frac{r^2}{2b^2} m_c d\dot{\theta} \\ -\frac{r^2}{2b^2} m_c d\dot{\theta} & 0 \end{bmatrix}, \quad \bar{T} = \begin{bmatrix} 1 & 0 \\ 0 & 1 \end{bmatrix}$$

Take $m = m_c + 2m_\omega, I = m_c d^2 + 2m_\omega b^2 + I_c + 2I_m$. The robot mass is taken as m_c = 10kg, d=0.3m, r=0.05, b=0.15m. The mass of a single driving wheel and motor is m_ω =1kg, and the moment of inertia of the robot for the longitudinal symmetry axis is $I_c = 4.625kg \cdot m^2$; The moment of inertia of a single drive wheel together with the motor for the drive wheel shaft $I_\omega = 0.0016kg \cdot m^2$; The moment of inertia of a single drive wheel together with the motor for the drive wheel diameter $I_m = 0.0004kg \cdot m^2$.

The parametric equation $\begin{cases} x_d = \cos t \\ y_d = \sin t \end{cases} (t \geq 0)$ for the expected trajectory is a circular trajectory. The design parameters of the controller in this paper are $k_1 = 50, k_2 = 50, k_3 = 50, K = 15, \Lambda = diag(10,10), \chi = 0.01$, and the external disturbance $\tau_d = [0.1\sin t, 0.1\cos t]$. The initial pose is $q = [0 \quad 0 \quad 0]^T$, the expected linear velocity is $v_r = 0.2m/s$, and the expected angular velocity is $v_r = 0.35rad/s$.

A. *Wheel no skid condition*

To compare the tracking performance of the control scheme designed in this paper under non-slip conditions, we first contrast it with adaptive sliding mode control applied in the absence of slipping.

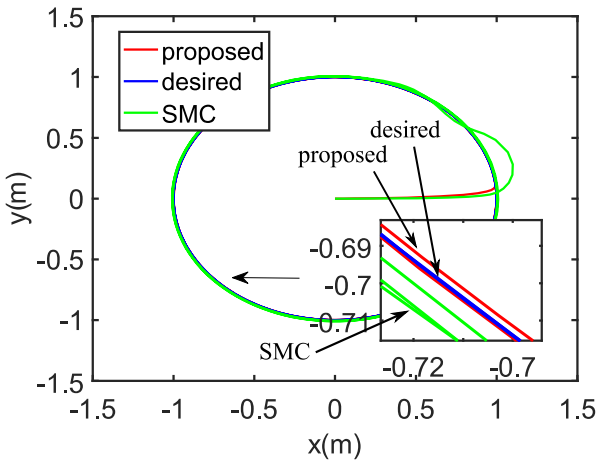

Fig. 5 Circular trajectory tracking

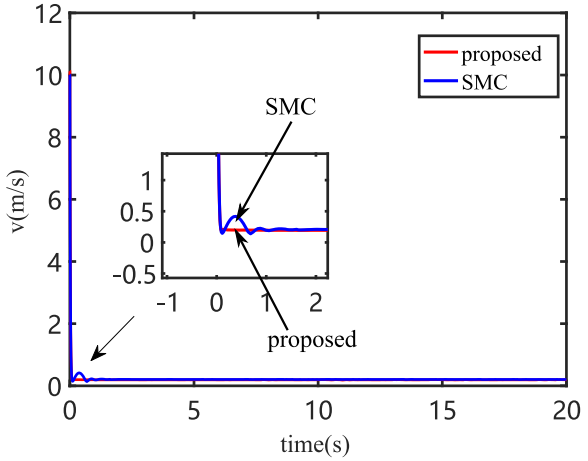

Fig. 6 Linear velocity tracking

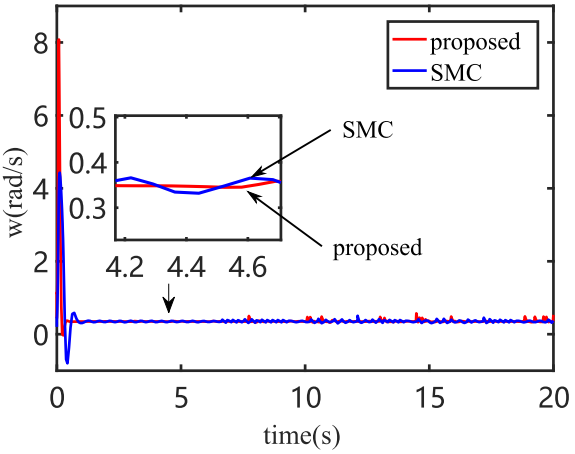

Fig. 7 Angular velocity tracking

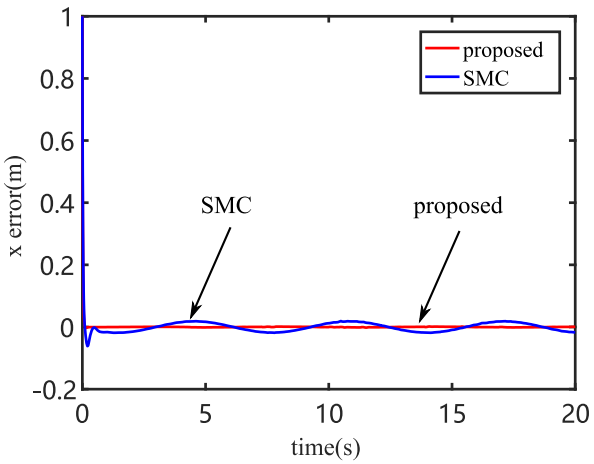

Fig. 8 X-axis direction error

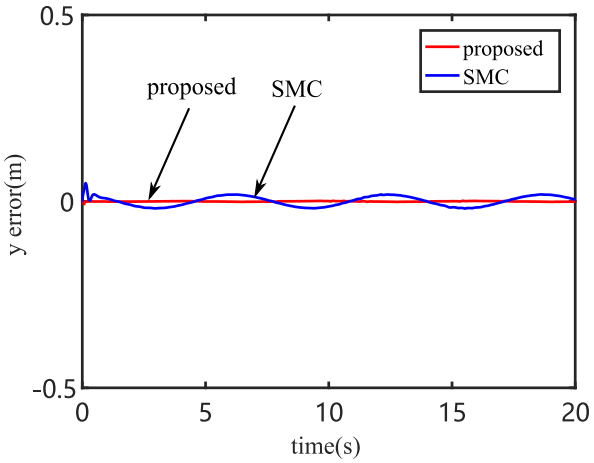

Fig. 9 Error in y direction

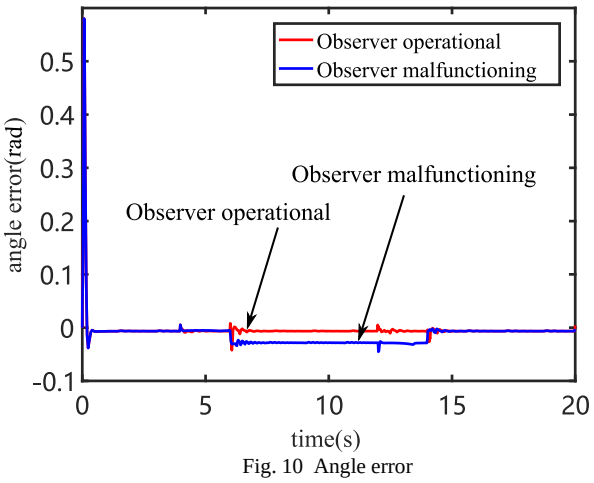

Fig. 10 Angle error

Fig.5 and Fig.8- Fig.10 demonstrate the tracking performance of two control schemes for circular trajectories. Notably, the tracking error of the control scheme proposed in this paper converges rapidly to zero, showcasing a significant improvement over typical adaptive sliding mode control. Specifically, the maximum lateral error (x) achieves an accuracy of approximately 6×10^{-4}m, the longitudinal error (y) is 5×10^{-3}m, and the angular error is 5×10^{-3}m, whereas the maximum error precision of typical adaptive sliding mode control is approximately 0.01m. Additionally, our controller demonstrates remarkable advantages in tracking vehicle body velocity and angular velocity. Compared to adaptive sliding mode control, the vehicle body velocity and angular velocity can track the desired speed more swiftly, with reduced angular velocity fluctuations, as illustrated in Fig.6 - Fig.7. This contributes significantly to the stability of the vehicle.

B. Wheel skid condition

To validate the correctness of the control algorithm for tracking trajectories of mobile robots under slip conditions as discussed earlier, and to assess the system's robustness, the variation in slip ratios is assumed as follows:

1. Initially, the left wheel of the mobile robot has no slip ratio, which abruptly changes to 30% at t=6s, and then reverts to no slip at t=14s.

2. Initially, the right wheel of the mobile robot has no slip ratio, which abruptly changes to 20% at t=4s, and then reverts to no slip at t=12s.

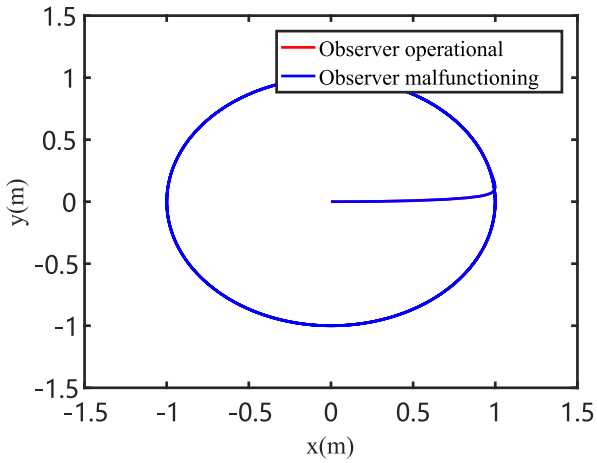

Fig. 11 Circular track tracking under skid conditions

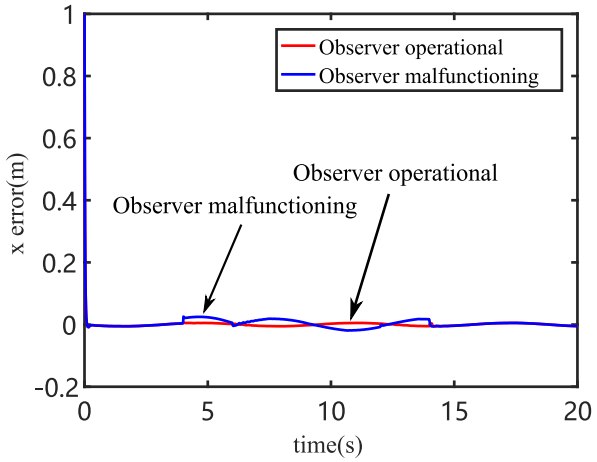

Fig. 12 X-axis error under skid conditions

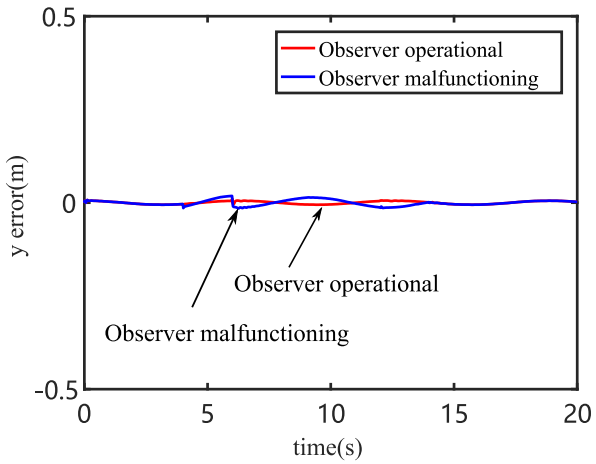

Fig. 13 Y-axis error under skid conditions

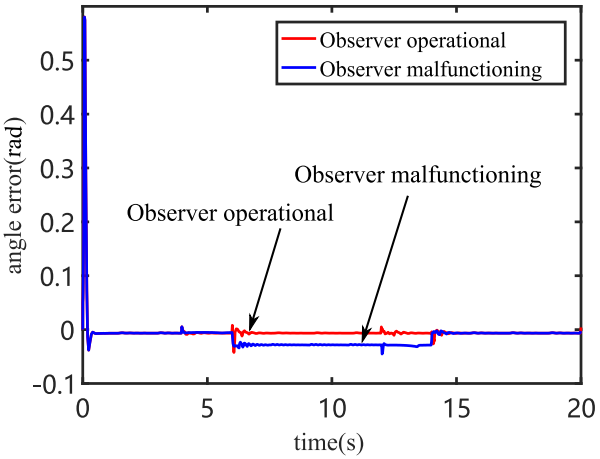

Fig. 14 Angle error under skid conditions

The reference trajectory of the mobile robot remains the parametric equation of a circular trajectory. The tracking performance of controlling after estimating the sliding parameters, as depicted in Fig. 11-14, surpasses that of direct control without estimation. From Fig. 12 and 13, it can be observed that the pose under direct control without estimation exhibits a deviation of approximately 0.02m in lateral and longitudinal errors after slipping occurs, although corrections are made under the control algorithm, the convergence of errors fluctuates significantly. In the second set of simulations, utilizing an observer for estimation before control reduces the deviation by half. Fig. 14 illustrates the angular error, where it is evident that in the first set of simulations, there exists a fixed deviation after slipping occurs, which cannot be corrected, with an error of approximately 0.035m. However, after estimating the sliding parameters before control, the angular error can converge in a short time, with the angular tracking accuracy improving to approximately 0.01m.

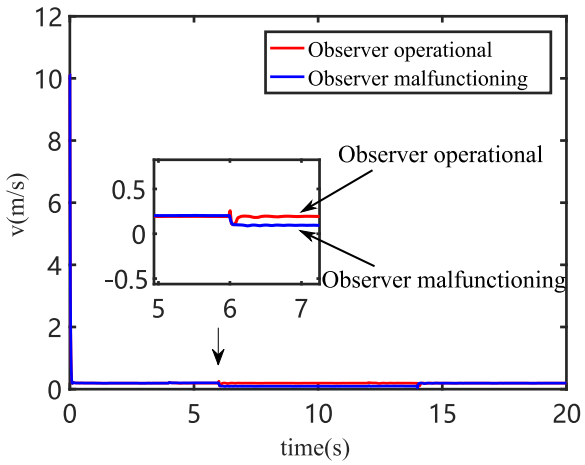

Fig 15 Iine speed tracking under skid conditions

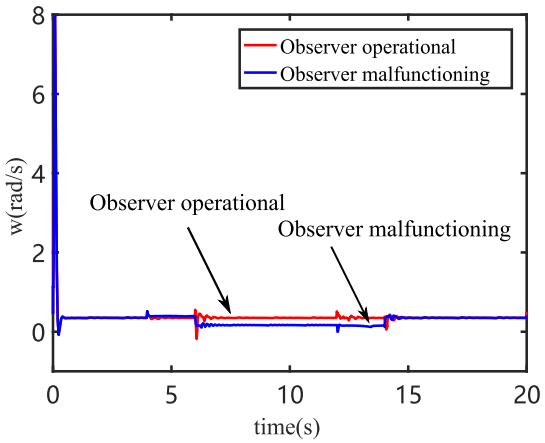

Fig 16 Angular velocity tracking under skid conditions

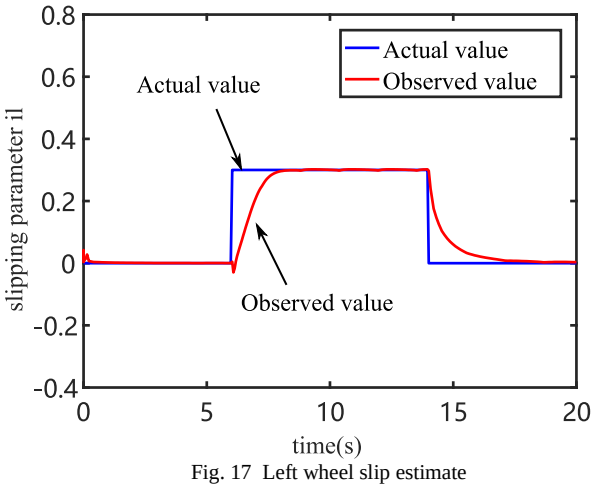

Fig. 17 Left wheel slip estimate

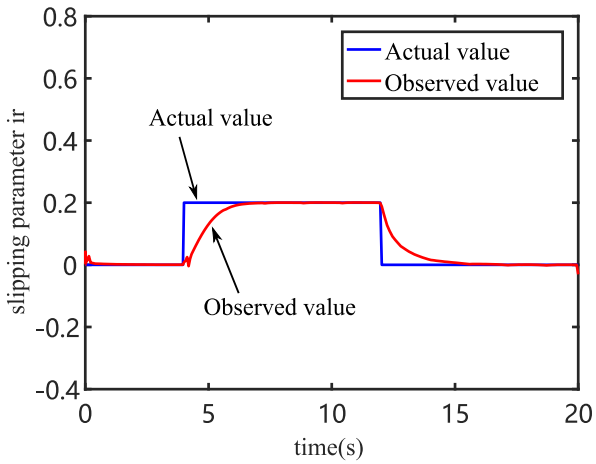

Fig 18 Right wheel slip estimate

The first set of simulations in Fig. 15 - Fig.16 exhibit similar trends in pose errors, where there exists a fixed deviation after wheel slippage occurs, which cannot be corrected. However, after estimating the sliding parameters before control, both the vehicle's linear and angular velocities can converge in a short time, tracking the desired velocities. Fig. 17 -Fig.18 depict the estimation results of the sliding parameters. It can be observed that both sliding parameters can be tracked to the actual slip parameters in a short time, with effective mitigation of disturbances caused by simultaneous slipping, demonstrating the effectiveness of the sliding mode observer for sliding parameter estimation.

VI. CONCLUSION

Addressing the stability control problem of wheeled mobile robots (WMR) under wheel slippage conditions, considering model parameter uncertainties and external disturbances, a FWNN control method based on a velocity observer is proposed. The following conclusions were drawn from the study: (1) By leveraging the relationship between slippage-induced pose deviations and the angular velocity equation, a sliding mode velocity observer was designed to achieve real-time estimation of velocity. (2) A FWNN compensator was designed to provide real-time compensation for uncertain models caused by parameter uncertainties and external disturbances. (3) A robust controller based on neural networks was designed using H∞ theory to ensure bounded control signals and system stability. Experimental validation confirmed the effectiveness of the proposed algorithm.

REFERENCE

[1] W Zhang, X Ye and X Ji, “RBF neural network adaptive control for space robots without speed feedback signal, ”Transactions of the Japan Society for Aeronautical and Space Sciences, vol.56, no.6, pp. 317-322, 2013

[2] L Jiang, W Zhang, J Shen, et al. “Vibration Suppression of Flexible Joints Space Robot based on Neural Network, ”IAENG International Journal of Applied Mathematics, vol.52, no.4, pp. 776-783, 2022

[3] W Zhang, J Shen, X Ye, et al. “Error model-oriented vibration suppression control of free-floating space robot with flexible joints based on adaptive neural network,”Engineering Applications of Artificial Intelligence, vol.114, no.4, 105028, 2022

[4] X Guo, W Zhang and F Gao, “Global Prescribed-Time Stabilization of Input-Quantized Nonlinear Systems via State-Scale Transformation ,” Electronics, vol.12, no.15, pp. 1-18, 2023

[5] Moosavian S A A, Kalantari A, “Experimental slip estimation for exact kinematics modeling and control of a tracked mobile robot” 2008 IEEE/RSJ International Conference on Intelligent Robots and Systems. IEEE, pp. 95-100, 2008.

[6] L Gracia and J Tornero, “Kinematic modeling of wheeled mobile robots with slip, ”Advanced Robotics, vol.21, no.11, pp. 1253-1279, 2007

[7] P Muir and C Neuman, “Kinematic modeling for feedback control of an omnidirectional wheeled mobile robot, ”Autonomous Robot Vehicles, pp. 25-31, 1990

[8] S Nandy, S Shome, R Somani, et al. “Detailed slip dynamics for nonholonomic mobile robotic system, ” 2011 IEEE International conference on mechatronics and automation. IEEE, pp. 519-524. 2011

[9] Y Wang, Y Jia, X Li, et al. “Dynamics modeling of a mobile manipulator for wheel slip avoidance, ” 2011 IEEE International Conference on Robotics and Biomimetics. IEEE, pp. 1621-1626. 2011

[10] G Wang, X Liu, Y Zhao, et al. “Neural network-based adaptive motion control for a mobile robot with unknown longitudinal sliping, ”Chinese Journal of Mechanical Engineering, vol.32, no.1, pp. 61, 2019

[11] T Nguyena, T Hoang, M Pham, et al. “A Gaussian wavelet network-based robust adaptive tracking controller for a wheeled mobile robot with unknown wheel slips, ” International Journal of Control, vol.92, no.11, pp. 2681-2692, 2019

[12] W Zhang, H Li, X Ye, et al. “Adaptive robust control for free-floating space robot with unknown uncertainty based on neural network, ”International Journal of Advanced Robotic Systems, vol.15, no.6, pp. 1-11, 2018

[13] J Shen , W Zhang, S Zhou, et al. “Fuzzy Adaptive Compensation Control for Space Manipulator with Joint Flexibility and Dead Zone Based on Neural Network, ”International Journal of Aeronautical and Space Sciences, vol.24, no.3, pp. 876-889, 2023

[14] W Zhang, F Gao, J Huang, et al. “Global Prescribed-Time Stabilization for a Class of Uncertain Feedforward Nonlinear Systems, ” IEEE Transactions on Circuits and Systems II: Express Briefs, vol.70, no.4, pp. 1450-1454, 2022

[15] Z You, W Zhang, J Shen, et al. “Adaptive neural network vibration suppression control of flexible joints space manipulator based on H∞ theory, ”Journal of Vibroengineering, vol.25, no.3, pp. 492-505, 2023

[16] W Zhang, X Ye and L Jiang, “Output feedback control for free-floating space robotic manipulators base on adaptive fuzzy neural network, ”Aerospace Science and Technology,vol.29, no.1, pp. 135–143, 2013

[17] L Yin, W Zhang, T Zhou, et al. “Machine Health-Driven Dynamic Scheduling of Hybrid Jobs for Flexible Manufacturing Shop,” International Journal of Precision Engineering and Manufacturing, vol.24, no.5, pp. 797-812, 2023

[18] W Zhang, N Qi and H Yin, “Neural-network tracking control of space robot based on sliding-mode variable structure, ”Control Theory and Applications, vol.28, no.9, pp. 1141-1144, 2011

[19] Y Hu and W Zhang, “Modeling framework for analyzing midair encounters in hybrid airspace where manned and unmanned aircraft coexist, ” Proceedings of the Institution of Mechanical Engineers, Part G: Journal of Aerospace Engineering, vol.233, no.15, pp. 5492-5506, 2019

[20] N Qi, W Zhang, J Gao, et al. “Design of Ground Simulation Test System for Three-dimensional Spatial Microgravity Environment, ”[J]. Journal of Mechanical Engineering, vol.47, no.9, pp. 16-20, 2011

[21] W Zhang, Y Shang Q Sun, et al, “Finite-Time Stabilization of General Stochastic Nonlinear Systems with Application to a Liquid-Level System, ”IAENG International Journal of Applied Mathematics, vol.51, no.2, pp. 295-299, 2021

[22] N Hoang and H Kang, “Neural network-based adaptive tracking control of mobile robots in the presence of wheel slip and external disturbance force, ”Neurocomputing, 188, pp. 12-22, 2016

[23] F Lin, H Shieh and P Huang, “Adaptive wavelet neural network control with hysteresis estimation for piezo-positioning mechanism, ” IEEE Transactions on Neural Networks, vol.17, no.2, pp. 432-444. 2006

[24] T Sun, H Pei Y Pan, et al. “Robust wavelet network control for a class of autonomous vehicles to track environmental contour line, ” Neurocomputing, vol.74, no.17, pp. 2886-2892, 2011

[25] W Zhang, X Ye, H Li, et al. “Robust Control for Robotic Manipulators Base on Adaptive Neural Network, ”The Open Mechanical Engineering Journal, vol.8, no.1, pp. 497-502, 2014

[26] Y Fang, W Zhang and X Ye. “Variable Structure Control for Space Robots Based on Neural Networks, ”International Journal of Advanced Robotic Systems, vol.11, no.3, pp. 35-42, 2014

[27] W Zhang, N Qi, J MA, et al. “Neural integrated control for free-floating space robot with changing parameters,” Science China: Information Science, vol.4, no.10, pp. 2091-2099, 2011

Linghong Zhu works as a associate professor in the School of Intelligent Manufacturing at Lishui Vocational and Technical College. He received a bachelor's degree in Mechanical Engineering and Automation and a master's degree in Mechanical Engineering from Zhejiang University of Technology in 2004 and 2011, respectively. His research interests include mechanical structure design optimization and intelligent control, robotics, mechatronics technology, etc.

Xiaochen Huang is currently a master's student at the School of Mechanical Engineering, Zhejiang Sci-Tech University. He received his bachelor's degree from Shanxi Institute of Technology in 2021. Her research focuses on mobile robot dynamics and control.

Xiaoming Wu works as a professor in the School of Intelligent Manufacturing at Lishui Vocational and Technical College. He received a bachelor's degree in Industrial Automation and a master's degree in Mechanical Manufacturing and Automation from Tongji University in 1990 and 1992, respectively. His research interests include industrial automation and intelligent control of equipment, new materials and mechatronics integration technology, etc.

Rui Chen is currently a master's student in the School of Mechanical Engineering at Zhejiang Sci-Tech University. He received his bachelor's degree from China Jiliang University College of Modern Science and Technology in 2021. His research focuses on nonlinear systems and automatic control.

Dajian Yi is currently a master's student at the School of Mechanical Engineering, Zhejiang Sci-Tech University. He received his bachelor's degree from Lishui University in 2022. Her research focuses on Machine Vision and Mechatronics Integration.

Wenhui Zhang works as a professor in the School of Electronic Engineering at Nanjing Xiaozhuang University. He received a bachelor's degree in Mechanical Design, Manufacturing, and Automation from Harbin Institute of Technology in 2004, a master's degree in Aerospace Engineering in 2008, and a PhD in Aerospace Science and Technology in 2011. His research interests include robotics technology and intelligent control, machine vision and mechatronics integration technology, etc.